Decadal variability of European sea level extremes in relation to the solar activity

Adrián Martínez-Asensio*[1,2], Michael N. Tsimplis[1,2], Francisco Mir Calafat[1]

[1] National Oceanography Centre, Southampton, UK
[2] School of Ocean and Earth Science, University of Southampton, Southampton, UK

*Corresponding author: a.martinez-asensio@soton.ac.uk

Abstract

This study investigates the relationship between decadal changes in solar activity and sea level extremes along the European Coasts and derived from tide gauge data. Autumn sea level extremes vary with the 11-year solar cycle at Venice as suggested by previous studies but a similar link is also found at Trieste. In addition, a solar signal in winter sea level extremes is also found at Venice, Trieste, Marseille, Ceuta, Brest and Newlyn. The influence of the solar cycle is also evident in the sea level extremes derived from a barotropic model with spatial patterns that are consistent with the correlations obtained at the tide gauges. This agreement indicates that the link to the solar cycle is through modulation of the atmospheric forcing. The only atmospheric regional pattern that showed variability at the 11-year period was the East Atlantic (EA) pattern.

1. Introduction

Sea level extremes pose risks for coastal cities and the coastal environment. Long-term changes in mean sea level (MSL) are expected to significantly amplify the impact of sea level extremes through the 21st century. These will operate in combination with decadal as well as shorter-term variations in the magnitude and frequency of sea level extremes. This paper focuses on the 11-year solar cycle. MSL changes over European coasts were found to be related to the 11-year sunspot cycle (Currie, 1981) with a lag of ~3.5 years caused by the solar modulation of the polar vortex of westerly winds (Kelly, 1977; Parker, 1976). Woodworth (1985) estimated the solar cycle signal in MSL to be between 1 and 1.5 cm also with a similar 3.5-year lag, in phase with the sunspot cycle over Southern Europe, and in anti-phase over Northern Europe**.** The North Atlantic Oscillation (NAO) accounts for the major part of the inter-annual and decadal variability of the westerly winds over Europe and a 11-year solar modulation of the NAO with a lag of a few years has been recently suggested (Gray et al., 2013; Scaife et al., 2013; Thieblemont et al., 2015) although the mechanisms explaining the solar influence on the troposphere are still unclear (Gray et al., 2010).

Sea level extremes have been reported in many studies to be changing in accordance with mean sea level changes. Therefore the changes in extreme sea level in Europe should include at least the 1-1.5 cm signal estimated by Woodworth (1985) for the 11-yr cycle. Sea level extremes over the European coasts are primarily related to the NAO (Tsimplis et al., 2005; Woodworth et al., 2007; Marcos et al., 2009; Tsimplis and Shaw, 2010) but other regional climate modes such as the Arctic Oscillation (AO), the East Atlantic pattern (EA), the East Atlantic Western/Russian Pattern (EA/WR) and the Scandinavian Pattern (SCAN) are also relevant (Menendez and Woodworth, 2010). However a significant relationship between sea level extremes and the 11-year solar cycle has been reported only at Venice (Punta della Salute) during the second half of the 20th century (Smith, 1986; Tomasin, 2002). Barriopedro et al. (2010) suggest, for Venice, that the interactions between the main regional climate modes during autumn favour the occurrence of sea level extremes during years of solar maxima while the opposite occurs during the solar minima. Both the studies of Tomasin (2002) and Bariopedro et al. (2010) involved a removal of the annual MSL prior to selecting the sea level extremes. Thus their results indicate that the 11-year cycle affects sea level extremes in Venice in addition to the influence it has on MSL. If the relationship between the 11-year cycle and extremes in Venice is caused by changes in the weather patterns one would expect to see a similar relationship in other tide gauge stations in the Mediterranean Sea and possible in other European coasts. Furthermore, in this latter case the solar cycle influence may also be, at least partly, captured by barotropic sea level models driven by wind and atmospheric pressure, and this would identify conclusively the physical forcing as of atmospheric origin though it will not resolve the link between solar activity and winds.

This study uses both the methodology developed by Tomasin (2002) and that developed by Barriopedro et al. (2010) to assess whether the observed contribution of the solar activity to sea level extremes in Venice can also be observed in other European tide-gauges. This relationship is evaluated by comparison of the sunspot number series (SSN) and a set of both observed and modelled sea level extremes series. The data sets and methods are introduced in section 2. Results are presented and discussed in section 3, and conclusions are provided in section 4.

2. Data set and methods

2.1 Data

Hourly sea level records for six long European tide gauge stations covering different periods are used. Three of the records (Ceuta, Brest and Newlyn) have been obtained from the University of Hawaii Sea Level Centre (UHSLC). Updated time series for Venice (Punta della Salute) and Trieste have been kindly provided by A. Tomasin and F. Raicich, respectively. The data for Marseille of Woppelmann et al (2014) has also been used. The locations and span of tide gauge stations are shown in Fig. 1. Five other UHSLC stations were also analyzed (La Coruña, Cuxhaven, Tregde, Gedser, Hornbaek, Stockholm and New York – see Fig. S1) but are not presented here because no correlation was found. However an explanation for the lack of correlation will be presented in the conclusions.

Atmospherically forced sea level values were obtained from the VANI2-ERA data set (Jordà et al., 2012). This dataset is based on a barotropic version of the HAMSOM model forced with atmospheric pressure and winds from a dynamical downscaling of the ERA40 reanalysis. The model output spans the period 1958–2008 and covers the Mediterranean Sea and a sector of the NE Atlantic Ocean with a spatial resolution of 1/6° x 1/4°. The model output (in this and earlier versions) have been used for estimations of sea level extremes in the Mediterranean (Marcos et al., 2009) and, despite their limitations (Calafat et al., 2015), provide valuable spatial information not available through observations. Monthly values of sunspot numbers were downloaded from the WDC-SILSO, Royal Observatory of Belgium, Brussels (http://sidc.oma.be/sunspot-data/SIDCpub.php).

2.2 Methodology

The extremes at these stations were estimated through the following process. Tidal residuals were first estimated by removing the tidal component from observations by use of the matlab UTide software (Codiga, 2011). MSL was filtered out from both the observations and the tidal residuals by use of a Butterworth high-pass filter of order 2 and 1 year cut-off period (Marcos et al., 2015). The mean annual and semi-annual components were also removed by fitting a regression model with two harmonics. The resulting time series were then used to calculate monthly values for two sea level extreme indicators. The first indicator used was the total number of hours of sea level (HSN) above a threshold. This indicator is related to the magnitude and frequency of storm surges. This is similar to the methodology used by Tomasin (2002) with the difference that we use the 99.5th percentile whereas Tomasin (2002) used a threshold of 0.50 m. The second indicator is a time series of the total number of independent sea level extreme events (ESN) per month, that is, the number of exceedances over the same threshold (99.5th percentile). This indicator, which was used by Barriopedro et al. (2010) albeit with a slightly different threshold (95th percentile), is a measure of the frequency of surge events and does not take in account their magnitude. For the computation of ESN a 72 hours minimum separation between successive events was used to ensure that the selected extreme events were approximately independent.

Only months having at least 50% of valid hourly values have been used for the calculation of the monthly time series of HSN and ESN. Annual values (from July to June) of the two indicators as well as seasonal values for autumn October-December (OND) and winter December-March (DJFM), respectively were computed from the monthly time series and will be the basis of the analysis. Seasonal values were produced when, at most, 1 monthly value was missing. The HSN and ESN time series for Venice are shown as an example in Fig. S2 and the seasonal data series for all stations in Figure S3. A low-pass filtered time series was also obtained for each indicator by applying a three-year running mean to the annual values. Analogous time series were obtained for the sunspot numbers (SSN) by annually and seasonally averaging the monthly time series of SSN.

The relationship between the sea level extremes and SSN was explored on the basis of the correlation values between the corresponding annual (OND, DJFM and the three-year running mean) anomalies of each variable during their overlapping periods. For the tide gauges, correlations were also calculated over the model period (1958-2008) for comparison. All time series were previously linearly detrended over the common period.

The statistical significance of the correlation coefficients between SSN and the extreme indices was calculated by using a randomization technique. Each hourly sea level extremes time series was first randomly permuted (with replacement) to build an ensemble of 500 time series. Then, for each time series in the ensemble 3-year low-pass filtered and seasonal (OND, DJFM) time series of both HSN and ESN were computed using the same procedure as for the original time series. The 3-year filtering period was selected in order to reduce high frequencies while retaining the 11-year cycle. Finally, the ranking of the correlation for the original time series within the sample of correlations derived from the randomized series was used as a measure of the statistical significance. The same procedure was used for the 2-D model values at each grid point. An alternative randomisation process preserving seasonality was also used and led to almost identical results.

3. Results

3.1 Relationship between solar cycle and storm surges

Significant correlations for autumn (OND) between sea level extremes and SSN were found for Venice (0.28 and 0.29, HSN and ESN, respectively) and Trieste (0.36 and 0.14, respectively) (Table 1). This is consistent with the findings of Barriopedro et al., 2010. Note that if the last HSN value of Venice is removed, as suggested by a reviewer, the correlation increases to 0.41.

For the winter season significant correlations between HSN and SSN were found at Venice (0.28), Trieste (0.29), Marseille (0.24) and Newlyn (0.32) over their overlapping periods. The low-pass filtered HSN time series show higher correlations for Venice (0.56), Trieste (0.45) and Newlyn (0.40) (see Table 1). This result is consistent with that shown in previous studies where a solar effect in HSN is suggested at Venice (0.67) during 1940-2006 for 3-year low-pass filtered time series (Tomasin, 2002; Pirazzolli and Tomasin, 2008). ESN at Ceuta (-0.29) and Brest (0.15) are also correlated to SSN. Lagged correlations (1-year) resulted in higher values for autumn correlations at all tide gauges (see Table S1), suggesting a possible lagged response to the forcing associated with the solar cycle.

The barotropic model provides the opportunity to conform the source of the correlation and enables the analysis of the corresponding spatial patterns of the correlation coefficients between SSN and storm surges for the Mediterranean and the Iberian coasts. Significant positive correlations between autumn (OND) SSN and HSN were found over all the northern part of the model domain (above 42ºN latitude) including both the NE Atlantic and the North Adriatic Sea with values of up to 0.38 (see Fig. 3a). These values are similar to those found for the observed HSE at both Venice (0.42) and Trieste (0.36) tide gauges over the same period (see Fig. 2). Significant correlations were also found for ESN over limited areas of both western and eastern basins with correlation values of up to 0.52 (see Fig. 3b) although no significant correlations were found over the NE Atlantic. During winter, significant correlations between SSN and HSN of up to 0.50 were found over all the northern part of the model domain (above 40N latitude) including both the NE Atlantic and the Mediterranean Sea (see Fig. 3c). This is consistent with the significant correlation (0.33) found for the tide gauge record of Marseille over the same period (see Fig. 2). Significant negative correlations of up to -0.34 between SSN and ESN were found in winter at limited areas over the Alboran Sea (see Fig. 3d) which is consistent with the correlation of -0.32 found at the tide gauge of Ceuta during the same period (not shown).

No significant correlations between the sunspot cycle and sea level extremes were found over the Atlantic coasts at latitudes lower than ~44ºN and ~42ºN for autumn and winter, respectively. This is consistent with the lack of correlation with SSN at the La Coruña tide gauge; the only tide gauge located inside the model domain that was not presented here (see Fig. S1).

The way the atmospheric forcing is linked to the sunspot cycle is unclear. To investigate this issue, we obtained composites of sea level pressure, winds, HSN and ESN anomalies for the periods of high (or low) solar activity during 1958-2008 corresponding to the three-year period of relative maximum (or minimum) SSN values (see Figs. S4a-h and supplementary text S1 in the supporting information). The composites associated with periods of high solar activity (see Figs. S4a-d) show a low pressure anomaly over Europe with its centre of action located over the North Sea

(English Channel) during autumn (winter) that favours the entrance of storms from the Atlantic (Rogers, 1990) and enhances the duration of storm surges over the Biscay Bay and the Mediterranean Sea during autumn (up to 6 hours on average) and winter (up to 8 hours on average) (see Figs. S4a, c). The increase in the cyclonic activity under periods of solar maxima also induces an increase in the frequency of the number of events over the Eastern Mediterranean during autumn (up to 0.3 events per month on average) (see Figs. S4b). One possible explanation for the correlation between SSN and of in HSN at the Atlantic coasts but not in ESN (see Figure 3) is that storms tend to last longer in the Atlantic than in the Mediterranean Sea, thus leading to more intense and longer surges in the former region. On the other hand, depressions in the Mediterranean Sea are more frequent which results in a larger number of surges (Trigo and Davies, 1999, Cid et al., 2016).

During the periods of low solar activity the opposite situation occurs. A positive pressure anomaly located over Europe with the potential to generate blocking events prevents the transport of mild air from the Atlantic into the continent and inhibits the storm track activity (Trigo et al., 2004; Sillmann and Croci-Maspoli, 2009; Mahlstein et al., 2012) over the entire domain in autumn (see Figs. S4e, f) and over the Atlantic and the Northern Mediterranean in winter (see Figs. S4g, h) which is consistent with the absence of correlation between SSN and the extremes in the Eastern Mediterranean (see Fig. 3d).

Large-scale atmospheric patterns have been suggested as the link between solar activity and mean sea level (Zanchettin et al. 2009) and extremes (Barriopedro et al., 2010) at Venice. We correlated the SSN with the NAO, the EA, the SCAN and the EA/WR patterns during the period 1871-2012. The winter EA is the only pattern that appears connected with the SSN with a low correlation value of 0.17 which is significant at the 94% confidence level. The power spectral density (PSD) of both the SSN and the winter EA index show significant energy at periods of about 11 years (Fig. S5) (see supplementary text S2 in the supporting information). We have tested the significance of the 11-year spectral peak against the background red noise from an AR1 process and have found that such peak reaches the 94.2% confidence interval for the red noise, suggesting that the peak is very likely real and not due to chance. The PSD of sea level extremes at Trieste also shows a maximum peak of energy at the 11-year period over 1939-2011 except for winter ESN, which is not surprising due to the lack of correlation found between this time series and the SSN (see Table 1). Note that we were not able to calculate the PSD at the rest of tide gauges due to the presence of gaps in the data.

The percentage of HSN and ESN variance accounted for by the climate indices and the SSN during the period 1958-2008 was quantified and averaged over the areas where the correlation with SSN is significant. The SSN accounts for a larger part of HSN and ESN variability than the climate indices with spatially averaged values of 9% (up to15% at certain locations) and 11% (up to 27%) for autumn, respectively, and 15% (up to 28%) and 9% (up to 11%) for winter. The climate indices account for a smaller fraction of the variance with values of 6% (up to 21%) by the EA in autumn HSN (1% by the NAO and the SCAN), 3% by the EA and the EA/WR in autumn ESN (2% by the NAO and 1% by the SCAN) and 5% by the SCAN in winter HSN (~2% by the rest of the indices). Note that the corresponding values for winter ESN are not discussed because they are not correlated to SSN. Although the SSN accounts for a larger fraction of the variance than climate indices, it is important to recognize that, first its influence is important for the specific period, thus for the interannual variability in extremes the NAO is the dominant pattern and, second, that the variance values are small (maximum values of 28% at some locations) and other drivers may play a more important role.

The composites associated with the positive (negative) phase of the EA pattern calculated over 1958-2008 show a low (high) pressure anomaly over most of the domain (see Figs. S4i-p) and resembles the composite associated with high (low) solar activity albeit with some differences in the location of the centres of action and the pressure gradients. The atmospheric composites did not significantly change when the 1871-2012 period was used. Positive (negative) EA phases are related to higher (lower) than average storm track activity coming from the Atlantic over the Bay of Biscay and the Northern Mediterranean (Woollings et al. 2010) and also to higher duration and frequency of surges specially during winter (see Figs. S4i-p). Similarities found between the different phases of the solar cycle and the EA pattern could explain the statistical relationship found between winter EA index and SSN.

4. Conclusions

We have investigated the decadal changes in sea level extremes along European coasts associated to the 11-year solar cycle. Our results confirm that the autumn extremes at Venice have variability at the sunspot cycle frequency as presented by Tomasin (2002) and Barriopedro et al., (2010). We further support these findings by confirming that similar results are obtained for nearby Trieste. Significant correlations are also found for winter at Venice and Trieste but also at Marseille, Ceuta, Brest and Newlyn. Through the analysis of an atmospherically forced barotropic model we confirm that solar activity is significantly related to the magnitude and frequency of storm surges at several locations along the European coasts. The spatial patterns derived from the model analysis are consistent with the correlations established at the tide gauges used in this study. The good agreement between the observed and modelled time series of HSN and ESN indicates a good ability by the model to capture the solar signal and suggests that the atmospheric forcing of the model included the 11-year period, which in turn lead to changes in sea level extremes. The identified changes in extremes are in addition to 1 – 1.5cm changes in MSL identified by earlier works. We found that the EA is the regional pattern that has variability at the 11-year period and also correlates with the extreme indicators variability at this periodicity. The sunspot cycle accounts for an important fraction of year-to-year variations of sea level extremes over the Mediterranean Sea and the NE Atlantic, with values of up to 28% of the interannual variability. Given the quasi-periodicity of the 11-year solar cycle our results can help to improve decadal predictions of sea level extremes over the highly populated coasts along the Mediterranean Sea and the NE Atlantic.

Acknowledgements

A. Martínez-Asensio, M. Tsimplis and F. M. Calafat acknowledge Lloyd's Register Foundation, which supports the advancement of engineering-related education, and funds research and development that enhances safety of life at sea, on land and in the air. We thank the University of Hawaii Sea Level Center (http://uhslc.soest.hawaii.edu/datainfo/) for providing us tide gauge data. We thank the Royal Observatory of Belgium (http://www.sidc.be/silso/datafiles) and NOAA (http://www.esrl.noaa.gov/psd/data/20thC_Rean/) for providing the sunspot number and 20th Century Reanalysis, respectively. We thank Marta Marcos for providing tide gauge data from Marseille and for the valuable help and technical support. We thank Alberto Tomasin (ISMAR-CNR) and Fabio Raicich (ISMAR-CNR) for providing tide gauge data from Venice and Trieste, respectively. We also thank Gabriel Jordà (IMEDEA-CSIC) for providing the modelled sea level fields. The authors would like to acknowledge comments received from Dr Thomas Wahl and an anonymous reviewer which led to significant improvements of the paper.

References

Barriopedro, D., R. García-Herrera, P. Lionello and C. Pino, 2010. A discussion of the links between solar variability and high-storm-surge events in Venice. J. Geophys. Res, 115, D13101.

Calafat, F. M., E. Avgoustoglou, G. Jordá, H. Flocas, G. Zodiatis, M. N. Tsimplis, and J. Kouroutzoglou, 2014. The ability of a barotropic model to simulate sea level extremes of meteorological origin in the Mediterranean Sea, including those caused by explosive cyclones. Journal of Geophysical Research: Oceans, 119(11), 7840-7853.

Cid, A., Menéndez, M., Castanedo, S., Abascal, A. J., Méndez, F. J., and Medina, R. 2016. Long-term changes in the frequency, intensity and duration of extreme storm surge events in southern Europe. Climate Dynamics, 46(5-6), 1503-1516.

Codiga, D. L., 2011. Unified tidal analysis and prediction using the UTide Matlab functions, Tech. Rep. 2011-01, 59 pp., Grad. Sch. of Oceanogr., Univ. of R. I., Narragansett. (Available at ftp://www.po.gso.uri.edu/pub/downloads/codiga/pubs/2011Codiga-UTide-Report.pdf)

Gray L. J., A. A. Scaife, D. Mitchell, S. Osprey, S. Ineson, S. Hardiman, N. Butchart N, J. Knight, R. Sutton, and K. Kodera, 2013. A lagged response to the 11-year solar cycle in observed winter Atlantic/European weather patterns. J. Geophys. Res. Atmos. 118, 13405-13420

Ineson, S., A. A. Scaife, J. R. Knight, J. C. Manners, N. J. Dunstone, L. J. Gray, and J. D. Haigh, 2011. Solar forcing of winter climate variability in the Northern Hemisphere. Nature Geoscience, 4(11), 753-757.

Jordà, G., D. Gomis and E. Álvarez-Fanjul, 2012. The VANI2-ERA hindcast of sea-level residuals: atmospheric forcing of sea-level variability in the Mediterranean Sea (1958–2008). Sci. Mar. 76, 133–146.

Kelly, P. M., 1977. Solar influence on North Atlantic mean sea level pressure, Nature, 269, 320-322.

Mahlstein, I., Martius, O., Chevalier, C., and D. Ginsbourger, 2012. Changes in the odds of extreme events in the Atlantic basin depending on the position of the extratropical jet. Geophysical Research Letters, 39(22).

Marcos, M., M. N. Tsimplis, and A. G. P. Shaw, 2009. Sea level extremes in southern Europe, J. Geophys. Res., 114, C01007.

Marcos, M., F. M. Calafat, Á. Berihuete, and S. Dangendorf, 2015. Long-term variations in global sea level extremes. Journal of Geophysical Research: Oceans, 120, 8115–8134.

Menéndez, M., and P. L. Woodworth, 2010. Changes in extreme high water levels based on a quasi-global tide-gauge data set, J. Geophys. Res., 115, C10011

Parker, B. N., 1976. Global pressure variation and the 11-year solar cycle, Met. Mag., 105, 33-44.

Pirazzoli, P. A. and A. Tomasin, 2008. Sea level and surges in the Adriatic Sea are: Recent trends and possible near-future scenarios. Atti Istituto Veneto di Scienze, Lettere ed Arti, CLXVI, 61–83.

Rogers, J. C., 1990. Patterns of low-frequency monthly sea level pressure variability (1899-1986) and associated wave cyclone frequencies. Journal of Climate, 3(12), 1364-1379.

Sillmann, J., and M. Croci-Maspoli, 2009. Present and future atmospheric blocking and its impact on European mean and extreme climate. Geophysical Research Letters, 36(10).

Thieblemont, R., K., M. Matthes, N. O. Omrani, K. Kodera, and F. Hansen, 2015. Solar forcing synchronizes decadal north atlantic climate variability. Nature Communications 6, 8268.

Tsimplis M. N., D. K., Woolf, T. J. Osborn, S. Wakelin, J. Wolf, R. A. Flather, A. G. P. Shaw, P. L. Woodworth, P. Challenor, D. L. Blackman, F. Pert, Z. Yan, S. Jevrejeva, 2005. Towards a vulnerability assessment of the UK and northern European coasts: the role of regional climate variability. Philos Trans R Soc Lond A 363(1831):1329–1358.

Tsimplis, M. N., and A. G. P. Shaw, 2010. Seasonal sea level extremes in the Mediterranean Sea and at the Atlantic European coasts, Nat. Hazards Earth Syst. Sci., 10, 1457-1475.

Tomasin, A., 2002. The frequency of Adriatic surges and solar activity, ISDGM Tech. Rep., 194, 1–8.

Trigo, I. F., Davies, T. D., and G. R. Bigg, 1999. Objective climatology of cyclones in the Mediterranean region. Journal of Climate, 12(6), 1685-1696.

Trigo, R. M., Trigo, I. F., DaCamara, C. C., and T. J Osborn, 2004. Climate impact of the European winter blocking episodes from the NCEP/NCAR Reanalyses. Climate Dynamics, 23(1), 17-28.

Welch, P. D., 1967. The use of Fast Fourier Transform for the estimation of power spectra: A method based on time averaging over short, modified periodograms, IEEE Transactions on Audio and Electroacoustics, AU-15 (2): 70–73.

Woodworth, P. L., 1985. A world-wide search for the 11-yr solar cycle in mean sea-level records. Geophysical Journal of the Royal Astronomical Society,80(3), 743-755.

Woodworth, P. L., and D. L. Blackman, 2002. Changes in extreme high waters at Liverpool since 1768. International journal of climatology, 22(6), 697-714.

Woodworth, P. L., Flather R. A., Williams, J. A., Wakelin, S. L. and S. Jevrejeva, 2007. The dependence of UK extreme sea levels and storm surges on the North Atlantic Oscillation. Continental Shelf Research, 27 (7). 935-946.

Woollings, T., Hannachi, A., and B. Hoskins, 2010. Variability of the North Atlantic eddy-driven jet stream. Quarterly Journal of the Royal Meteorological Society, 136(649), 856-868.

Zanchettin, D., A. Rubino, P. Traverso, and M. Tomasino, 2009. Teleconnections force interannual-to-decadal tidal variability in the Lagoon of Venice (northern Adriatic), J. Geophys.Res., 114, D07106.

Table and Figure Captions

Table 1. Correlation coefficients between annual (OND, DJFM, and 3-year running mean) SSN and both HSN and ESN at tide gauge stations during the overlapping period (left). Correlation coefficients at their corresponding closest model grid points are also listed (marked by asterisk). Boldface values denote statistical significance at 0.05% level.

Figure 1. Map showing the location of tide gauge stations and period of operation.

Figure 2. Standardized annual time series of total number of surge hours (blue lines) and sunspot number (red lines). Autumn (OND) time series are plotted for Venice and Trieste while winter (DJFM) time series are plotted for the rest of stations. Plotted time series of Ceuta are multiplied by -1. Correlation coefficients calculated during the overlapping periods (r1) and during the period 1958-2008 (r2) are shown. Asterisks denote statistical significance at 0.05 level.

Figure 3. Correlation coefficients between modelled annual time series of SSN and both HSN and ESN during 1958 - 2008 for autumn (a, b) and winter (c, d). Black line denotes statistical significance at a 0.05 level.

Table 1. Correlation coefficients between annual (OND, DJFM, and 3-year running mean) SSN and both HSN and ESN at tide gauges stations during the overlapping period (left). Correlation coefficients at their corresponding closest grid points are also listed (marked by asterisk). Boldface values denote statistical significance at 0.05% level.

	OND		DJFM		3-year running mean	
	HSN	ESN	HSN	ESN	HSN	ESN
Venice	**0.28**	**0.29**	**0.28**	0.02	**0.56**	0.29
Venice *	**0.34**	**0.39**	**0.46**	0.11	**0.61**	**0.45**
Trieste	**0.36**	0.14	**0.29**	0.05	**0.45**	0.18
Trieste *	**0.32**	**0.41**	**0.47**	0.14	**0.58**	0.37
Marseille	0.14	0.05	**0.24**	0.05	0.22	0.01
Marseille*	0.23	**0.30**	0.26	0.03	0.36	0.16
Ceuta	0.03	0.05	-0.13	**-0.29**	-0.14	-0.20
Ceuta*	0.00	0.01	-0.05	-0.19	-0.01	-0.14
Brest	0.12	0.07	0.15	**0.15**	0.16	0.11
Newlyn	0.18	0.06	**0.32**	0.19	**0.40**	0.20

Figure 1.

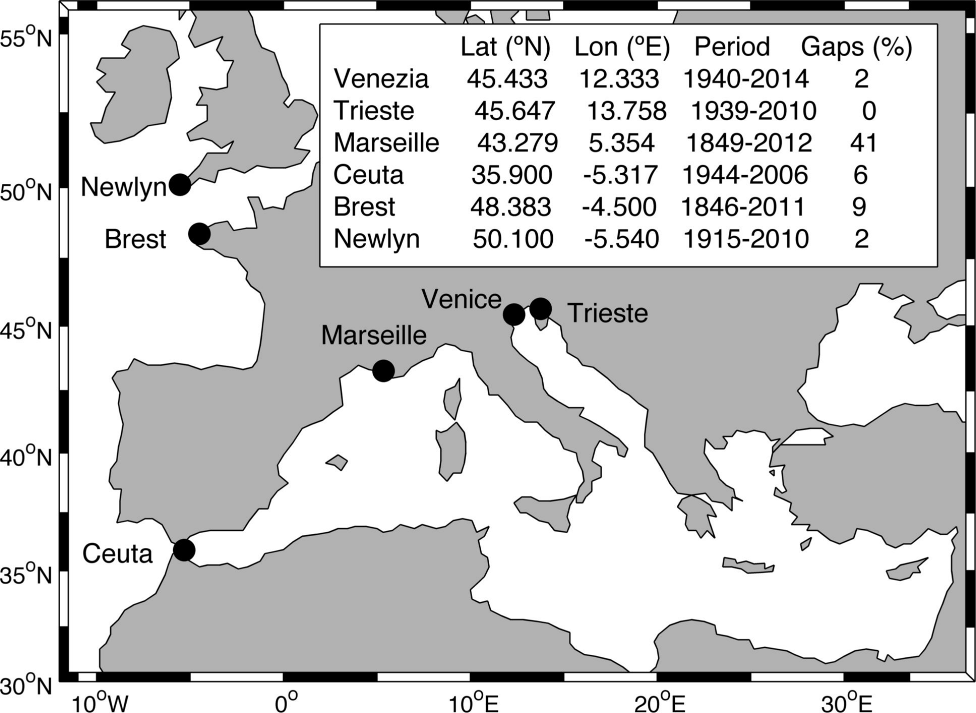

Lat (ºN) Lon (ºE) Period Gaps (%)
Venezia 45.433 12.333 1940-2014 2
Trieste 45.647 13.758 1939-2010 0
Marseille 43.279 5.354 1849-2012 41
Ceuta 35.900 -5.317 1944-2006 6
Brest 48.383 -4.500 1846-2011 9
Newlyn 50.100 -5.540 1915-2010 2
Newlyn
Brest
Venice
Trieste
Marseille
Ceuta
55ºN
50ºN
45ºN
40ºN
35ºN
30ºN
10ºW
0º
10ºE
20ºE
30ºE

Figure 2.

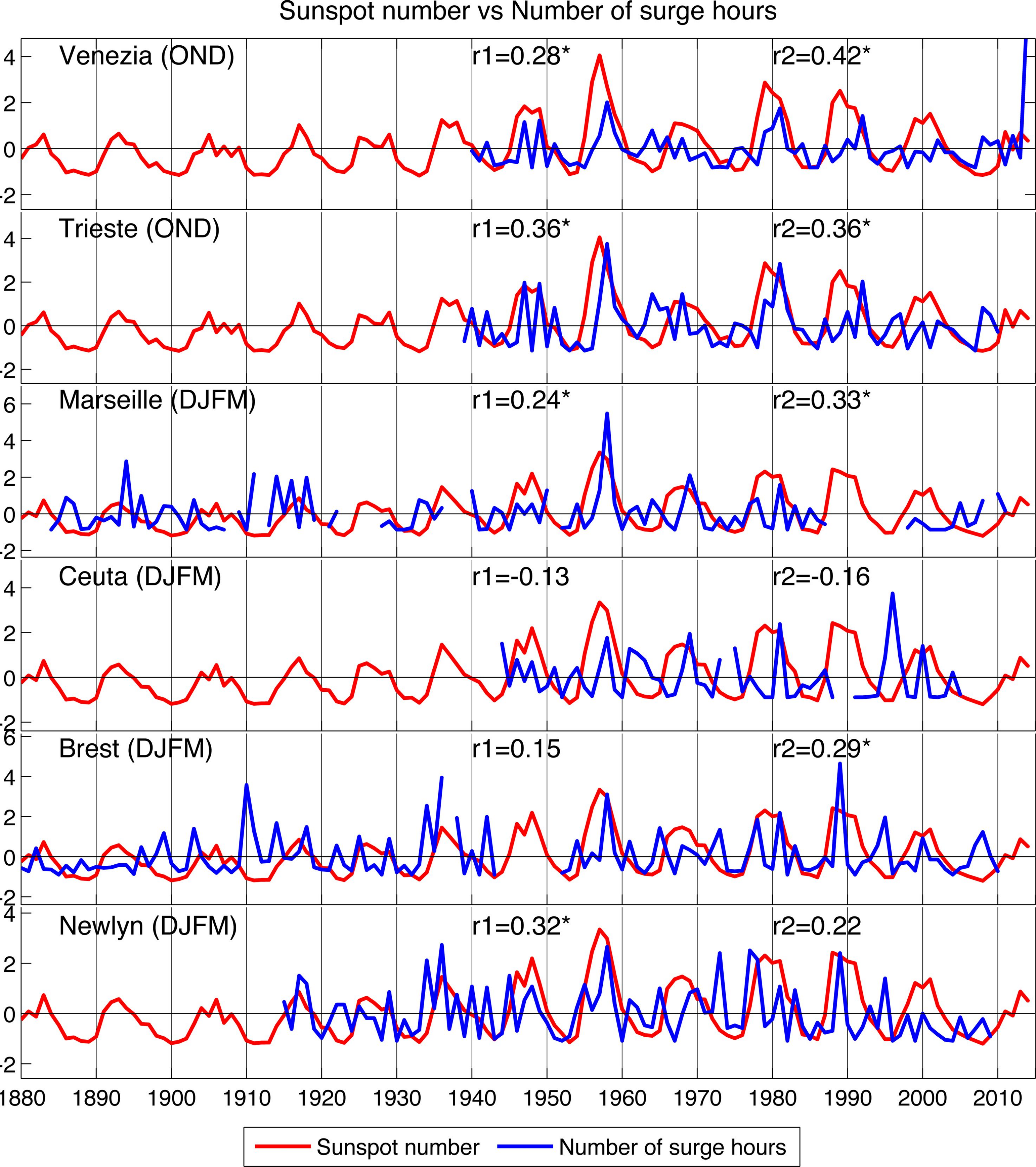
Sunspot number vs Number of surge hours
Venezia (OND)
r1=0.28*
r2=0.42*
Trieste (OND)
r1=0.36*
r2=0.36*
Marseille (DJFM)
r1=0.24*
r2=0.33*
Ceuta (DJFM)
r1=-0.13
r2=-0.16
Brest (DJFM)
r1=0.15
r2=0.29*
Newlyn (DJFM)
r1=0.32*
r2=0.22
1880
1890
1900
1910
1920
1930
1940
1950
1960
1970
1980
1990
2000
2010
Sunspot number
Number of surge hours

Figure 3.

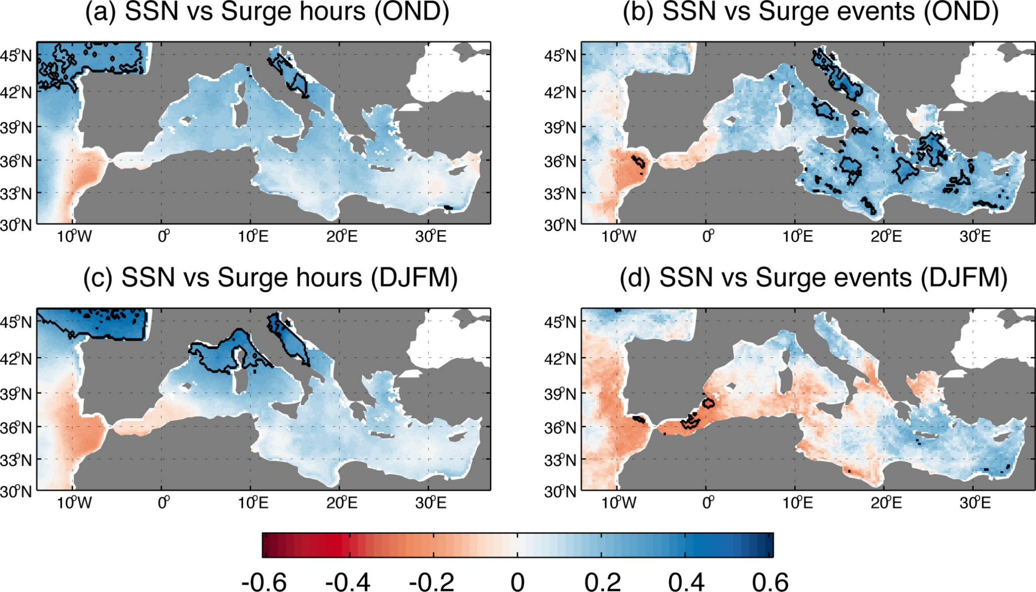

(a) SSN vs Surge hours (OND)
(b) SSN vs Surge events (OND)
(c) SSN vs Surge hours (DJFM)
(d) SSN vs Surge events (DJFM)
45°N
42°N
39°N
36°N
33°N
30°N
10°W
0°
10°E
20°E
30°E
-0.6
-0.4
-0.2
0
0.2
0.4
0.6

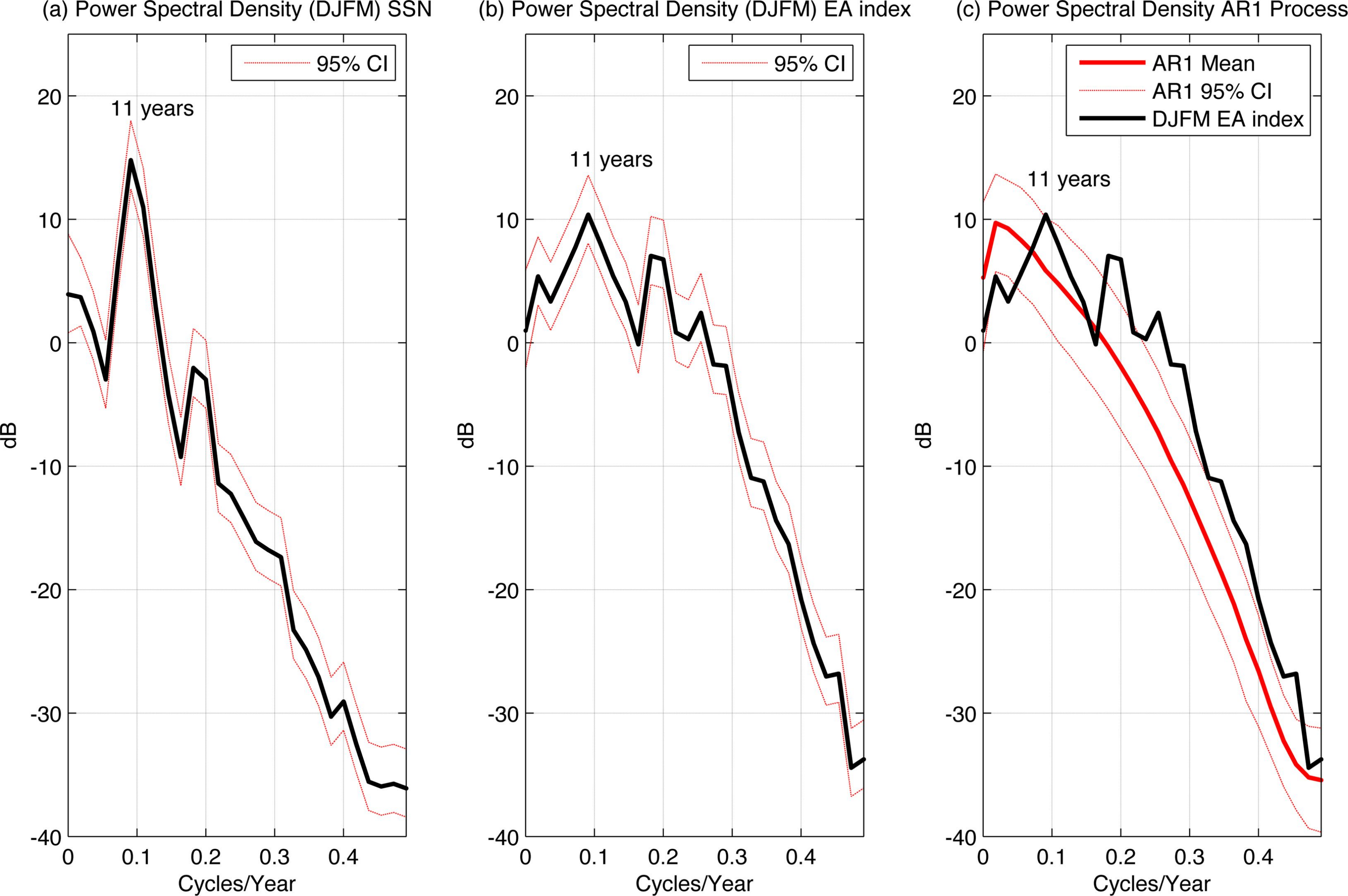

(a) Power Spectral Density (DJFM) SSN
95% CI
11 years
dB
Cycles/Year
(b) Power Spectral Density (DJFM) EA index
95% CI
11 years
dB
Cycles/Year
(c) Power Spectral Density AR1 Process
AR1 Mean
AR1 95% CI
DJFM EA index
11 years
dB
Cycles/Year
20
10
0
-10
-20
-30
-40
0
0.1
0.2
0.3
0.4

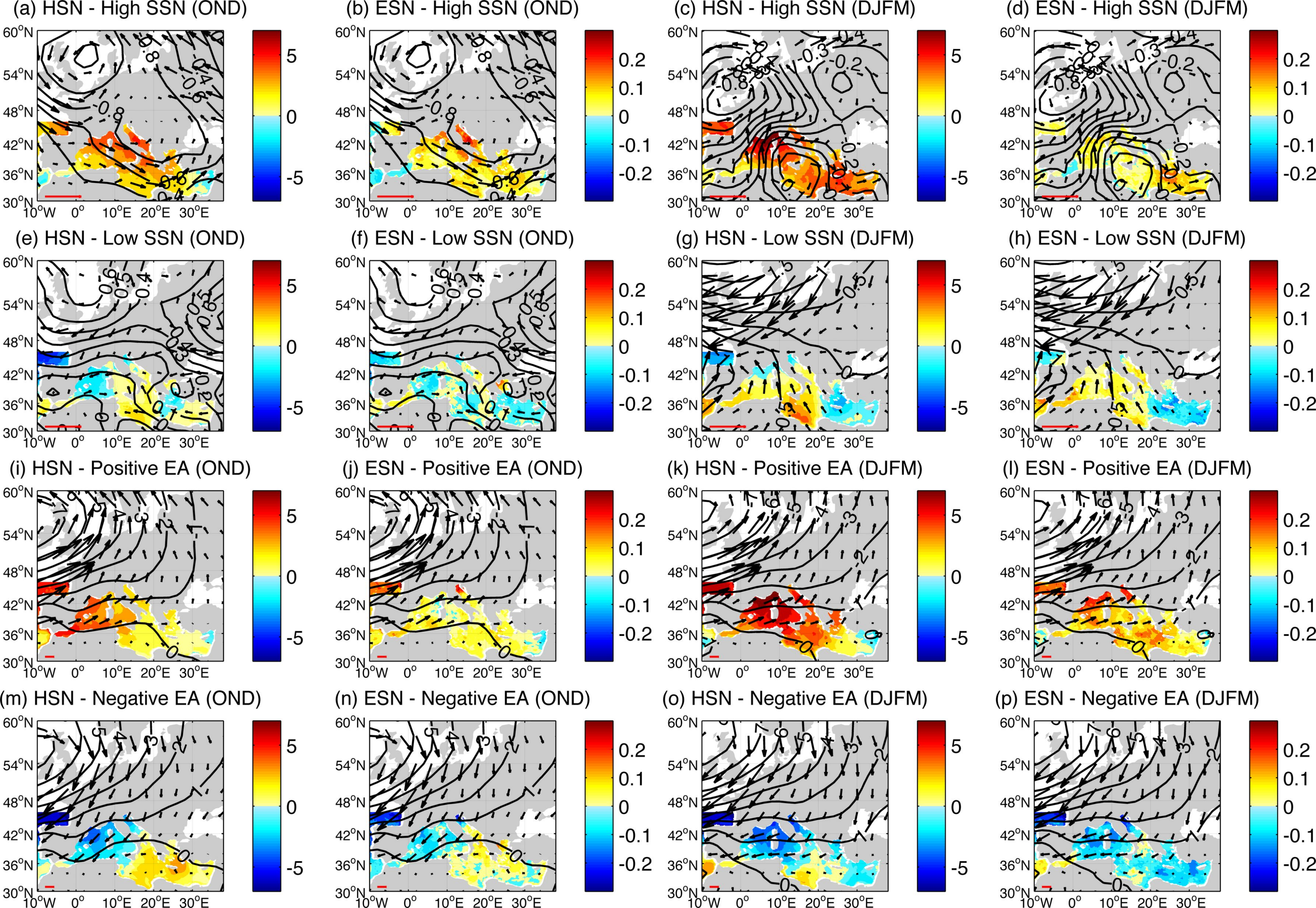
(a) HSN - High SSN (OND)
(b) ESN - High SSN (OND)
(c) HSN - High SSN (DJFM)
(d) ESN - High SSN (DJFM)
(e) HSN - Low SSN (OND)
(f) ESN - Low SSN (OND)
(g) HSN - Low SSN (DJFM)
(h) ESN - Low SSN (DJFM)
(i) HSN - Positive EA (OND)
(j) ESN - Positive EA (OND)
(k) HSN - Positive EA (DJFM)
(l) ESN - Positive EA (DJFM)
(m) HSN - Negative EA (OND)
(n) ESN - Negative EA (OND)
(o) HSN - Negative EA (DJFM)
(p) ESN - Negative EA (DJFM)